256 | https://doi.org/10.3311/PPch.21253

Periodica Polytechnica Chemical Engineering, 67(2), pp. 256–270, 2023

Fabrication, Characterization and Permeation Studies of Ionically Cross-linked Chitosan/Kaolin Composite Membranes

Sonia Bouzid Rekik[1,2,3*], Sana Gassara[1], Jamel Bouaziz[2], Semia Baklouti[4], Andre Deratani[1]

[1] European Institute of Membranes (IEM), University of Montpellier, Place Eugène Bataillon, Cedex 5, 34095 Montpellier, France
[2] Laboratory of Advanced Materials, National School of Engineering, University of Sfax, P. O. B. 1173, 3038 Sfax, Tunisia
[3] Bioengineering, Tissues and Neuroplasticity, EA 7377, Faculty of Health, Université Paris-Est Créteil Val de Marne, 8 rue du Général Sarrail, 94010 Créteil, France
[4] Laboratory of Materials Engineering and Environment, National School of Engineering, University of Sfax, P. O. B. 1173, 3038 Sfax, Tunisia
* Corresponding author, e-mail: sonia.rekik@u-pec.fr

Received: 28 September 2022, Accepted: 17 January 2023, Published online: 09 March 2023

Abstract

This paper presents the successful preparation of porous membranes based on chitosan with enhanced mechanical, thermal and chemical properties applicable in water treatment field. Herein, chitosan/kaolin composite membranes with a cross-linking agent and a porogen were prepared using the solvent casting method. The characterization of the as-fabricated membranes indicated that the combined effect of kaolin as reinforcing agent, polyethylene glycol as pore former and citric acid as cross-linker in a chitosan matrix showed a significant influence on the membrane properties. The results indicated that the incorporation of a hydrophilic porogenic reagent into the collodion in addition to providing a porous morphology makes it possible to obtain a more hydrophilic membrane, and thus induces an increase in the pure water permeability. The cross-linked membranes exhibited an improved water resistance, better thermal and mechanical properties as compared to neat chitosan films. The cross-linked membranes had a mean pore size of 50 nm falling in the range of ultrafiltration. Their functional properties were determined in terms of pure water filtration and molecular weight cut-off tests.

Keywords

ultrafiltration membrane, biopolymer/inorganic mixed matrix, citric acid, pore size determination

1 Introduction

Membrane filtration is one among the most promising technologies for water treatment application. The most commonly used polymers for membrane manufacture are fossil fuel-based synthetic polymers, which are also non-biodegradable [1, 2]. The increasing environmental pollution and the nearby depletion of fossil fuels has been the starting point for the research of potential natural polymers that can replace the conventional polymers for membrane preparation. In this direction, the use of biodegradable and biocompatible materials as membrane matrix is one of the major criteria to be considered [3–5]. In this context, there is a growing interest in biopolymers derived from animal and plant sources, as well as bacterial fermentation products, in parallel with the increasing worldwide trend towards sustainability. Chitosan (CS) is an attractive choice since it represents a good balance between human food consumption and valorization of industrial by-products. Chitin, the acetylated precursor form of CS, is naturally occurring in the wall of fungi, exoskeletons of crustacean and insects. CS has many applications in pharmaceutical and biomedical fields due to its remarkable properties such as biodegradability, biocompatibility and anti-bacterial properties [6–9]. Moreover, CS as a membrane material has attracted the interest of many researchers worldwide because of its good film-forming ability, hydrophilicity, cationicity and ease of modification [10, 11]. So far, the use of chitosan has been widely explored in the preparation of adsorbent membranes, pervaporation membranes and for drug delivery applications [12–16]. However, the potential of this polymer in the preparation of membranes applicable in water and wastewater treatment has not been much studied. Pure

Cite this article as: Rekik, S. B., Gassara, S., Bouaziz, J., Baklouti, S., Deratani, A. "Fabrication, Characterization and Permeation Studies of Ionically Cross-linked Chitosan/Kaolin Composite Membranes", Periodica Polytechnica Chemical Engineering, 67(2), pp. 256–270, 2023. https://doi.org/10.3311/PPch.21253

CS film shows some shortcomings in terms of mechanical strength, thermal stability and solubility properties, which limits its use in water treatment [12, 17–19]. Hence, due to the tendency of CS to dissolve at pH below 5.5, chitosan-based membrane cannot be used in acidic solutions. In addition, the poor mechanical stability of this material in the wet state has severely hampered its widespread use. Another weakness of CS that must be taking into account, is the dense structure of the membranes obtained making it difficult the application for liquid filtration.

Several strategies have been developed to overcome these limitations including the preparation of composite membranes with mixed CS/inorganic or polymeric matrices and/or a cross-linking of CS [17, 18, 20–26]. In an acidic environment, CS molecules are positively charged due to protonation of amino groups along the CS backbone [27]. The cationic character of CS in acidic conditions offers the possibility of establishing electrostatic interactions with other negatively charged compounds [15, 20]. In this sense, chitosan with reactive functional groups in its backbone can be used for the preparation of composite membranes. The incorporation of inorganic materials bearing anionic charges into the CS matrix is a promising route to address the above issues by combining the advantages of organic polymer materials and inorganic materials. A variety of inorganic clays like montmorillonite, bentonite, saponite, kaolin (KO) etc. has been investigated to play this role [20, 23–31]. The incorporation of these fillers has improved the mechanical, thermal and chemical stability of the resulting composite. However, the effect of kaolin-clays on physico-chemical and permeation properties of chitosan-based membranes has not been investigated, especially in the context of water treatment application [32, 33]. Recently, novel CS/KO composite membranes have been developed in our team by the combination of solvent casting and evaporation process, which significantly improved the thermal, mechanical and chemical properties compared to the neat CS membrane [17]. However, low permeability and low surface porosity are the main drawbacks of this composite membrane which limits its application in water treatment and reduces the membrane lifetime. Furthermore, it was demonstrated that the prepared membranes could retain its original state in deionized water, but dissolved and lost their structure in acidic media. Thus, to overcome of this problem, CS needs to be cross-linked to make the membrane insoluble and allow further use in water. Furthermore, cross-linking can enhance the mechanical strength and thermal stability of membranes [19, 34, 35]. On the other hand, the properties of a membrane such as its hydrophilicity and porous structure have a great influence on its performance [36, 37]. Hence, achieving high permeability, high surface porosity and good pore structure of membranes is very crucial. The present work is therefore an extension to our previous study, where CS/KO composite membranes were developed [17]. As mentioned above, the porosity and chemical stability of the obtained membrane can be regulated by the addition of porogens as well as cross-linkers. In this paper, polyethylene glycol (PEG) was used as a hydrophilic additive to simultaneously generate the porosity and improve the hydrophilicity of membranes. In order to impart better stability to the membranes, they were cross-linked using citric acid (CA). CA is an environmentally friendly, nontoxic compound and has been used previously as an efficient cross-linking agent for polysaccharides [19, 38, 39]. CA is a low molecular weight polyfunctional bio-based starting material that contains two reactive primary carboxylic groups, one sterically hindered hydroxyl group and one less reactive tertiary carboxylic group. The negatively charged carboxylate groups can interact with the cationic chitosan by electrostatic forces. It is obvious that the incorporation of cross-linkers and porogens will also affect other properties of the base membrane.

Based on the above background, the fabrication of CA cross-linked-CS/KO/PEG composite to comply with membrane technology applications is quite attractive and to the best of our knowledge there is no related report, yet. Thus, the present work investigates the effect of incorporating CA cross-linker and PEG pore generator on the properties of CS/KO composite membranes. The physicochemical and functional properties of the membranes were studied and compared with that of neat chitosan films. In addition, the effect of CA as cross-linking agent on membrane properties including water flux, hydrophilicity, PEG rejection and pore size distribution was studied and the results were discussed.

2 Experimental

2.1 Material

Chitosan (CS), with a mass average molecular weight of 180.000 g/mol and a degree of deacetylation of 80% was obtained from France Chitine. The clay used in the present study was a Codex kaolin (KO) provided by the L.P.M Cerina (Laboratoire des Plantes Médicinales, Tunisia). Polyethylene glycol (PEG, M_W = 10000 g/mol) was purchased from Fluka and used as the pore forming polymeric additive in the casting solutions while citric acid (CA) was

obtained from Sigma-Aldrich and used as a cross-linker. Acetic acid and sodium hydroxide pellets were laboratory grade chemicals. Polyethylene oxide (PEO, M_W 100 and 300 kDa) purchased from Fluka and Polyethylene glycol (PEG, M_W from 200 to 35,000 Da) from Sigma-Aldrich were used for membrane molecular weight cutoff (MWCO) characterization. Deionized (DI) water (18 MΩ/cm, Millipore Milli-Q) was used to prepare all aqueous solutions.

2.2 Composite membrane preparation

2.2.1 Composite slurry preparation

The pure CS solution and the composite CS/KO slurries were prepared following a procedure described in our previous work [17]. Firstly, the CS solutions were prepared by adding 4 g of CS into 100 mL acetic acid solution (0.1 M) and allowed to dissolve completely at room temperature. A determined amount of KO was then added slowly to the CS solution. The mass fraction of KO was adjusted to 5% (w/v). The mixtures were further stirred for 24 h at room temperature to ensure a complete homogenization. In order to induce porosity, PEG powder was added to the previously obtained slurry under stirring to yield the dope suspension named as CS/KO/PEG. In our previous publications [17, 18], it has been found that the optimal KO mass fraction was 5% (w/v) and the optimal PEG mass fraction was 1% (w/v).

2.2.2 Cross-linking

The cross-linking reaction in CS/KO/PEG solutions was performed with CA. This reaction creates electrostatic bonds between CS chains under acidic conditions in order to consolidate the structure and to make the polymer insoluble in water and in acidic medium. CA (0.5 (w/v)) was added to the CS/KO/PEG composite systems in solution at 45 °C and stirred for 3 h before casting. Preliminary studies concluded that this mass fraction is required to produce membranes with desirable properties for water treatment applications. Table 1 shows the different compositions of the prepared dope mixtures.

Table 1 Composition of the studied dope mixture

Sample name	Chitosan powder (w/v)	Kaolin powder (w/v)	PEG powder (w/v)	CA powder (w/v)
CS	4	0	0	0
CS/KO	4	5	0	0
CS/KO/PEG (non-cross-linked)	4	5	1	0
CS/KO/PEG/CA (cross-linked)	4	5	1	0.5

2.2.3 Membrane casting

Fig. 1 shows the different steps of membrane preparation. The casting solution was carefully poured onto a glass-plate and followed by a casting operation with a 700 µm knife gap at room temperature. Then, the cast membrane was dried at room temperature to partially evaporate the solvents. Subsequently, the forming membranes were neutralized by immersing them into a 1 mol/l NaOH solution for 24 h. Treating the composite with NaOH was found to significantly improve the membrane resistance to water washout [40, 41]. Finally, the resulting substrate was washed in DI water to remove the excess NaOH and stored in DI water for later tests.

2.3 Membrane characterization

2.3.1 Viscosity measurements

To evaluate the cross-linking kinetics, the viscosity variation of pure CS collodions, the non-cross-linked and cross-linked solutions, was measured using a Physica MCR301 advanced cylinder rotary rheometer (Anton Paar). The influence of temperature on the dynamic viscosity of mixtures with different compositions was also determined. The temperature scan tests were performed in a range of 20 °C to 80 °C. All the measurements were performed based on the computer software Tool-master (an automatic measuring and accessory detection system) connected to the rheometer.

2.3.2 Scanning electron microscopy (SEM) analysis and pore size measurements

The surface and cross-section morphology of the obtained membranes was examined by scanning electron microscopy (SEM) (Hitachi S-4500, resolution of 1.5 nm at 15 kV). The samples were dried at room temperature, cut into small pieces and then coated with a thin layer of Pt by sputtering before SEM analysis. For cross-sectional image acquisition, the pieces were cryogenically broken

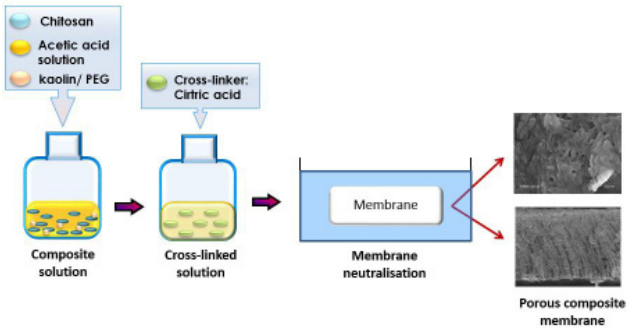

Fig. 1 Preparation procedure of CA-cross-linked chitosan/kaolin/PEG composite membrane

in liquid nitrogen. The mean pore size and pore size distribution were estimated from a selection of 5–8 pictures taken from pieces of at least three different membranes by treatment of the surface SEM pictures using Gwyddion 2.25 imaging analysis software.

2.3.3 Contact angle determination

The water contact angle (WCA) determines the hydrophilicity of the membrane and hence its water permeability performance. The sessile drop method with water droplets was applied for the surface analysis. Approximately 10 µL of DI water was deposited on the membrane surface using a micro syringe. The drop contour was analyzed using image analysis software (open source ImageJ software). The contact angle was then determined by interpolation methods (DropSnake plugin method). To minimize experimental error, the contact angle was measured at three random positions and their average values was reported.

2.3.4 Mechanical property measurements

The mechanical properties of the membranes were evaluated by extensional rheology. These tests were performed using a rheometer MCR 301 (Anton Paar) using a Universal Extensional Fixture UXF12. The temperature was controlled at 25 °C with a CTD180 Peltier system. The samples tested were 4 × 1 cm^2 rectangles cut in different parts of the membranes (at least 3 per formulation). This test was performed on the membrane in wet state. The wet state corresponded to a membrane being stored in water for more than 24 h.

2.3.5 Thermogravimetric analysis

Thermogravimetric analysis (TGA) of composite membranes with various additives was conducted using a TGA instrument (Hi-Res TGA 2950). This study provided important information on the thermal stability of the prepared membranes. The experiment was performed under a nitrogen atmosphere to prevent possible thermo-oxidative degradation. About 6 mg of the composite membranes were scanned from 25 to 800 °C at a heating rate of 10 °C/min.

2.3.6 Water solubility

The membrane solubility in water (natural pH), acidic (pH = 4) and basic (pH = 9) media was determined from the weight loss of the dry samples. It was defined by the content of dry matter solubilized after 24 h immersion into the considered medium. In brief, each membrane sample (20 mm × 20 mm) was dried in an oven at 80 °C until a constant weight was obtained, and then immersed into 50 mL of the equilibrium solution. After a contact of 24 h at room temperature, the pieces of membranes were taken out and dried to constant weight in an oven at 80 °C, to determine the weight of insolubilized dry matter. The measurement of the soluble fraction was determined as follows:

$$\mathrm{SOL} = \frac{M_i - M_f}{M_i} \times 100 \,, \tag{1}$$

where SOL is the percentage of soluble material, M_i and M_f are the initial and final sample mass, respectively.

2.3.7 Characterization of membranes by permeation experiments

Water filtration tests were performed using the Amicon Stirred Ultrafiltration Cell 8050 on flat membranes. The effective filtration surface area was 13.4 cm^2. The membranes were first conditioned in the test cell with pure water by gradually increasing the pressure to 4 bar for at least 3 h. All filtration experiments were carried out at an applied pressure in the range of 1–2 bar and a room temperature (25 °C).

Pure water flux (PWF) and Pure water permeability (PWP)

Membrane permeability is reported in terms of pure water flux (PWF) by circulating DI water through the membrane module. PWF (L/m^2 h) was calculated using the following expression:

$$\mathrm{PWF} = \frac{Q}{\Delta t \times A} = \mathrm{PWP} \times \Delta P \,, \tag{2}$$

where Q (L) is the permeate volume, Δt (h) is the permeation time, A (m^2) is the active membrane surface area, PWP (L/h m^2 bar) is the pure water permeability and ΔP (bar) is the transmembrane pressure. The pure water permeability PWP was determined from the slope of the linear variation of PWF as a function of applied pressure.

MWCO determination

MWCO is defined as the molecular weight of a neutral solute having a rejection higher than 90%. It was determined by using the rejection of neutral solutes (Polyethylene oxide PEO and Polyethylene glycol PEG) [42]. The single rejection experiments were conducted using 1 g/l aqueous solutions of model solutes (PEG and PEO) with different molecular weights. All experiments were conducted at room temperature with constant stirring at 2 bar. The system was thoroughly rinsed with DI water between

the different runs. First, the PWP of membranes was measured. Then the feed solution was introduced and the filtrate was collected at 2 bar. During this step, the filtration cell was stirred at 500 rpm to minimize concentration polarization. The membrane was then washed several times with DI water and PWP was measured again. The recovery of the initial PWP means that the membrane was not fouled during the solute transport experiments. The PEG/PEO contents in the feed (C_f) and in the permeate (C_p) solutions were determined by flow injection analysis using a refractometer 2414 (Waters Corporation). The solute rejection was calculated using Eq. (3):

$$R(\%) = \left(1 - \frac{C_p}{C_f}\right) \times 100 \tag{3}$$

in which C_p and C_f are the permeate and feed concentrations, respectively.

3 Results and discussion

3.1 Rheological properties of casting mixtures

In order to consolidate the structure and to make the polymer insoluble in acidic media, several routes of cross-linking have already been reported in the literature [19, 22, 25, 26, 34, 35, 38]. In our study it is crucial that the cross-linking reaction occurs during the membrane formation. Therefore, CA was added directly into the casting solution. Since it was necessary to add CA in the composite solution, the modification of the values of the viscosity was investigated using in-situ viscosity measurements. Fig. 2 shows the viscosity variation versus temperature of the different prepared casting solutions. For all compositions, the same evolution is observed,

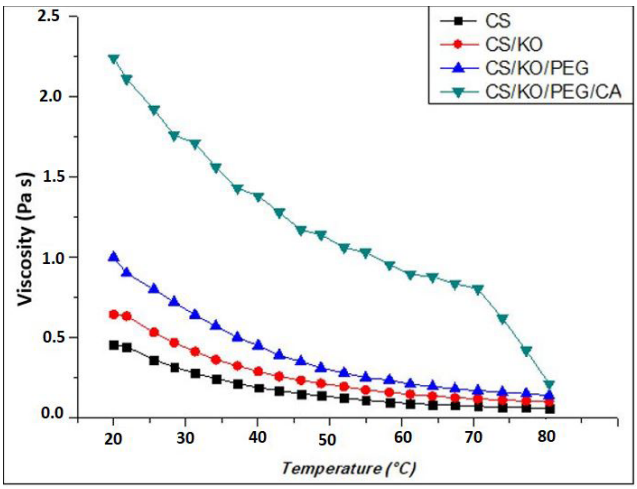

Fig. 2 Evolution of the viscosity with temperature for the different prepared solutions

with increasing concentration of additives a pronounced increase of the suspension viscosity can be observed. These results are in agreement with the values given in the literature [43, 44] and are generated by an increase in inter-particle and polymer interactions which due to the higher concentration of additives.

As observed, the addition of KO and PEG modified only slightly the viscosity values in contrast to the addition of CA. The former increase in the viscosity can be explained by the electrostatic interactions and hydrogen bonds that can take place owing to the existence of amino and hydroxyl groups on CS and anionic and hydroxyl groups on mineral particles (KO). However, these interactions have only a small impact on the viscosity indicating that there is no cross-linking reaction of CS chains but an intercalation of CS between the KO layers. The additional viscosity increase observed upon PEG addition probably originates from the insertion of PEG chains between the polymer chains and clays layers resulting in an increased mutual interaction between the particles. The sharp increase in viscosity upon CA addition seems to indicate a phase transition when enough cross-linking points, were created inducing a fixed structure limiting the polymer chain mobility [45]. The influence of temperature on the slurry viscosity was studied at varying temperatures ranging from 20 to 80 °C. As expected, an increase of temperature leads to a decrease in suspension viscosity because of chain relaxation at high temperature. As depicted in Fig. 2, a small change in temperature significantly impacted the cross-linking kinetics meaning that temperature should be carefully controlled. The effective cross-linking temperature was estimated when the maximum viscosity was reached after CA addition. It should be noted that a dramatic decrease in viscosity is observed above about 70 °C, which might be a ceiling temperature for the CA cross-linking reaction. Indeed, it can be seen that the viscosity at 80 °C is similar to that of the slurry without CA.

3.2 Characterization of the fabricated membranes

The present section aims at studying the effect of CA cross-linking on the membrane functional properties. Moreover, the effects of adding KO and PEG were also investigated. Indeed, our group has already reported on Chitosan-Kaolin composite membrane development where KO acted as a successful filler of CS, essential for enhancing mechanical, thermal and chemical stability [17]. Therefore, in this study, it was necessary to determine the compatibility of PEG addition with CA cross-linking and its effect on the resulting membrane properties.

3.2.1 Membrane morphology observation

The morphology of the synthetized membranes is a very important characteristic because it is directly responsible for many functional properties of the membrane. Fig. 3 shows the SEM images of the pure and modified CS membranes with different additive mass ratios. Fig. 3 illustrates the large differences between the neat CS membrane and all the modified membranes. The neat CS films have a continuous structure with a smooth, homogenous, and compact surface without pores or cracks. Fig. 4 shows a cross-section image of the same film, which indicates that the membrane structure is dense without any holes.

SEM images of the membrane surface with high magnification (×15K) allow us to observe that a well-defined and uniform pore structure successfully occurred for casting slurries containing both KO and PEG additives but was not achieved for the suspension containing only KO powder (Fig. 3). The CS/KO composite membrane shows a much rougher surface morphology than the pure CS membrane. As previously reported by Rekik et al. [17], a zoom of this composite membrane structure clearly reveals the existence of very small pores with a size that can be estimated to be between 20 and 60 nm by image analysis. It was assumed that the penetration and intercalation of the CS chains into the KO layers results in a three-dimensional network structure, which is mainly responsible for the formation of nano-sized pores in CS/KO composite membrane. SEM observations reveal that a small amount of polymeric pore-forming agent induced a large change of the membrane structure. As can be seen in Fig. 3, as expected, PEG acts as a porogen into the casting slurry composition giving rise to a significant pore opening and to a porosity increase. As a result, the membrane surface exhibits well-defined porous structure that can provide better conditions for enhanced permeability. These significant changes can be explained by the hydrophilic contribution of PEG to the CS matrix that splits the polymer chains and enlarges the interstices, thereby increasing the porosity [36]. In addition to the morphological improvements, the introduction of PEG can also improve the chemical properties of the CS/KO membranes by generating additional reactive functionalities (hydroxyl groups of PEG) into the membrane structure. Fig. 3 also shows the impact of the cross-linking step on the membrane structure. Careful observation of SEM micrographs shows that the cross-linked membranes have much narrower pores than the non-cross-linked membranes. Thus, it can be concluded that cross-linking significantly affects the pore size and pore density, indicating that negatively charged negatively charged COO-ions of cross-linking agent can easily diffuse into the interpenetrated CS/KO network. The negatively charged CA molecules probably replace some of electrostatic bonding between KO with CS chains, resulting in a tightening of the final network.

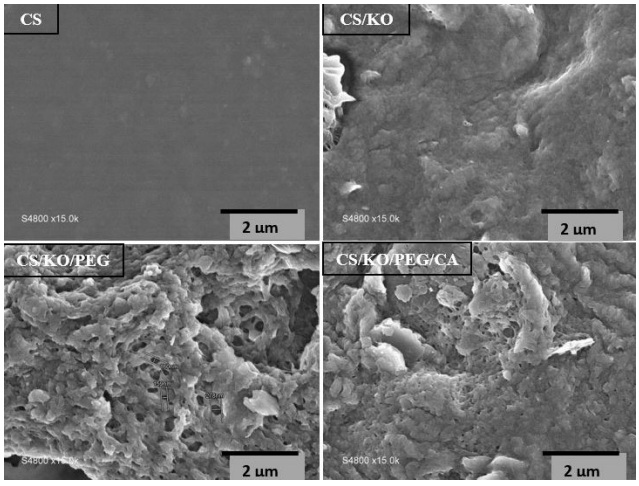

Fig. 3 SEM photographs of the surface of dense pure CS film, CS/KO composite membrane, non-cross-linked (CS/KO/PEG) and CA cross-linked membranes (magnification ×15k)

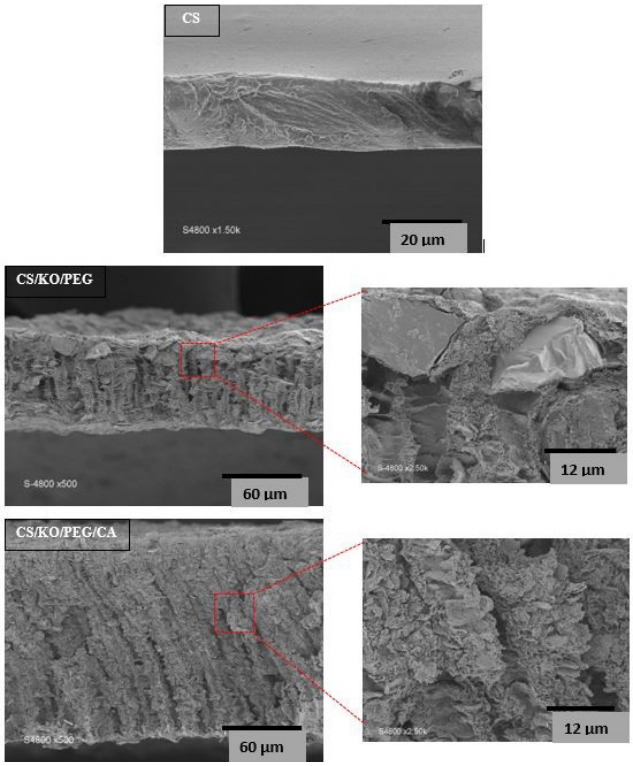

Fig. 4 SEM images of cross sections of pure chitosan film, non-cross-linked (CS/KO/PEG) and cross-linked membranes (CS/KO/PEG/CA) (magnification ×500)

Fig. 4 shows the effect of cross-linking-treatment on morphology by comparing the cross section of non-cross-linked and cross-linked membranes. The CS/KO/PEG membranes have a finger-like structure that almost completely crosses the membranes leading to good pore interconnectivity. Because PEG is water soluble, it is extracted from the forming membrane in the coagulation bath, resulting in an interconnected finger-like structure, which is similar to that observed when PEG is incorporated into other kinds of composite membranes [10, 37, 46]. Introduction of the cross-linking agent into the membrane matrix resulted in a narrower finger-like structure and thicker membrane. The structural change is evidence of the strong cross-linking reaction between CA with CS and confirms our previous assumption deduced from the membrane surface observation. From this behavior, it can be concluded that the carboxyl groups of CA involved in cross-linking lead to the restriction of the permeation channels and the reduction of the number and average pore diameter due to the high cross-linking density. The change in membrane thickness determined from the SEM observation of membrane cross sections is also shown in Fig. 4. There was a clear trend of increasing thickness with increasing additive concentration. In particular, the thickness of the cross-linked membrane was the highest (ca. 140 μm) of all samples compared to that of the pristine CS membrane (ca. 18 μm) and the non-cross-linked membrane (ca. 70 μm) indicating a higher porosity of its structure. The different cross-sectional and surface structure of the prepared membranes directly reflect on the physicochemical and transport membrane properties, which are presented in Section 3.2.3 and Section 3.3.

3.2.2 Pore size distribution (PSD)

Mean surface pore size and pores density present within the membranes are important parameters that determine flux and selectivity of membranes. The effect of cross-linking step on the pore size distribution (PSD) is demonstrated in Fig. 5.

SEM observation of the surfaces indicates that smaller pores were obtained using a formulation including CA. The average pore size was found to be 100 nm and 50 nm for CS/KO/PEG and CS/KO/PEG/CA, respectively. The pore size distribution of the non-cross-linked membrane between 9 and 520 nm, approximately. On the other hand, the pore size distribution of the cross-linked membrane appears to be narrower with values between 9 to 340 nm. Two conclusions can be drawn from the

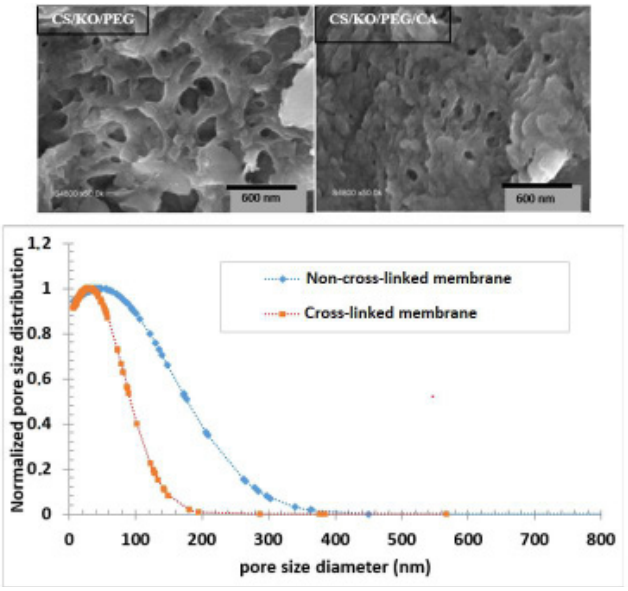

Fig. 5 Pore size distribution of non-cross-linked and cross-linked membranes

morphology analysis: first, the decrease of the mean pore size after the cross-linker addition and, second, a narrowing of the distribution indicating a high cross-linking density between CA and CS.

3.2.3 Hydrophilic properties of modified membranes

Contact angle experiments were performed using the static sessile drop method in order to better correlate the morphologies of the textured surfaces with the surface properties of all the modified membranes. Water is the best standard liquid to evaluate hydrophilic/hydrophobic properties of a surface. Fig. 6 shows the effect of additives on the change in surface water contact angle (WCA). The neat CS membrane exhibited a WCA value of 57°. Lower the values higher, the more hydrophilic the surface. Pristine CS based membrane tend to absorb water molecules because of the presence of N–H and O–H functional groups on the chains. The WCA value of the CS/KO composite membrane

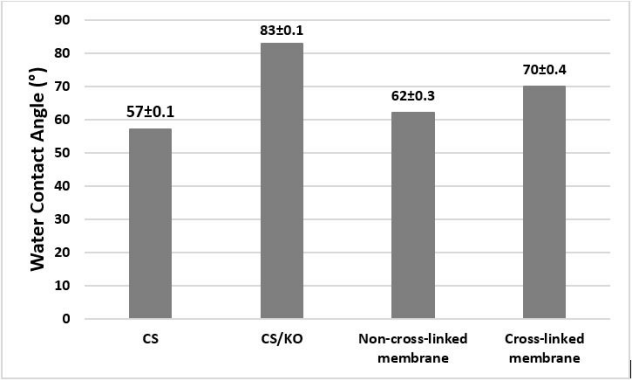

Fig. 6 Water contact angles of plain and composite membranes

is much higher than that of the pristine membrane indicating that these fillers confer greater hydrophobicity to the membrane surface. It has been previously shown that incorporating KO particles into the CS matrix could lead to hydrogen bonding interactions between the functional groups of KO and the amino ($–NH_2$) and hydroxyl (–OH) groups of CS in addition to the above-mentioned electrostatic interactions [17]. As a result, the hydrophilic moieties of CS molecules available for interaction with water molecules decreases. Compared to all the composite membranes, the non-cross-linked samples showed the lowest WCA value indicating a more hydrophilic surface. In contrast, the addition of CA increased the hydrophobicity giving a higher contact angle in the case of the cross-linked membranes. These findings can be explained in two ways. First, the observed decrease of WCA for CS/KO/PEG membranes indicated that the incorporation of PEG resulted in a better wettability of the obtained membrane. Probably, some PEG molecules remain trapped in the network in interaction with the other components. This effect might be due to the morphology change observed for the samples (see Section 3.2.1). The pore size and the porosity also increased by the addition of PEG, implying an increased surface area suitable for PEG sorption. PEG chains were able to physically combine with water molecules by H-bonding and thus increasing the hydrophilicity of membrane. This finding was similar to the results of You et al. [46] who reported a decrease in the WCA values of polyamide membrane after PEG incorporation. Second, during the cross-linking step in the preparation of composite membrane, the amino groups of CS react more with the carboxylic groups of CA, as mentioned above, due to its higher diffusivity related to its small size. Thus, the large extent of the cross-linking reaction caused a less availability of the CS hydrophilic groups and an increase in the membrane hydrophobicity. It is also important to emphasize that the physical cross-linked by the carboxylic groups changed the membrane structure and surface roughness (SEM and PSD data). Similar results have been reported by Priyadarshi et al. [19] for CS films cross-linked by citric acid.

It is well known that these two parameters can influence the accuracy of the contact angle measurement process [47]. Roughness of membrane surface was examined by SEM images at low magnification (×500) (Fig. 7). These observations agree well with the WCA results. Pure CS membrane exhibited the lowest surface roughness which is in agreement with its lower WCA. In the micrographs,

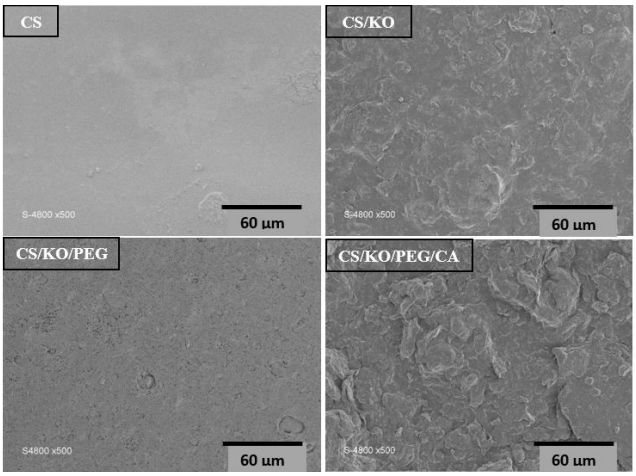

Fig. 7 SEM images of the as-fabricated membrane surfaces (magnification ×500)

it can be clearly seen that the surface morphology of the composite membranes after KO loading becomes rougher compared to that of neat CS membrane, again in agreement with the WCA data. As mentioned above and previously reported [17], the KO functional groups participate in hydrogen bonding interactions with the amino and hydroxyl groups of CS molecules, which reduces the interaction of the membrane with water molecules due to the lower availability of the hydrophilic CS molecule. On the other hand, the surface roughness also plays a key role in imparting an apparent hydrophobic character to the membrane surface. Aggregated particles can be seen evenly distributed on the surface of CS/KO composite membrane, which are mainly responsible for the observed surface roughness. As shown in Fig. 7, the addition of PEG to the casting solution leads to the formation of membranes with the smallest roughness and the most hydrophilic surface among all composite membranes. Comparatively higher surface roughness was observed for the cross-linked membranes. Higher surface roughness allows air to be trapped in the structure, thus preventing water from wetting the membrane surface as previously reported [35].

3.2.4 Membrane mechanical properties

Good mechanical properties of membranes in the wet state are one of the necessary requirements for their practical applications. The mechanical stability of unmodified and modified wet membranes was measured in terms of tensile strength and elongation at break (Fig. 8). As can be seen, the values of tensile strength and strain at break for pure CS membrane are smaller than those of all the composite membranes. The addition of KO to the CS matrix induced an enhancement of the mechanical properties.

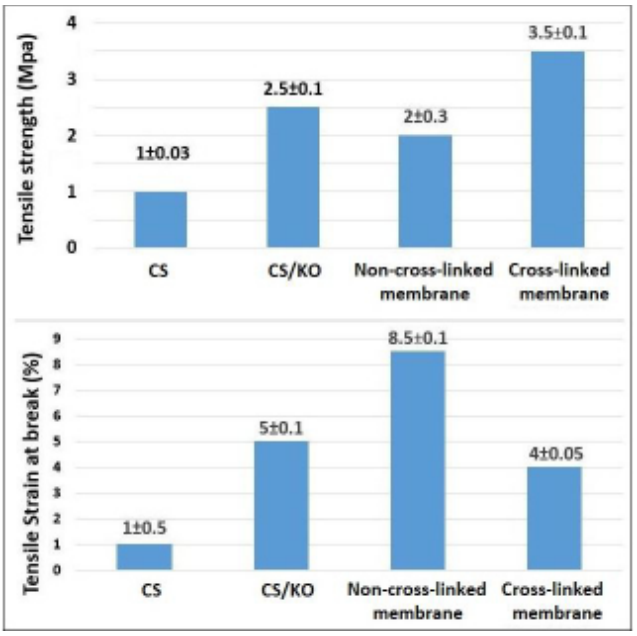

Fig. 8 Mechanical properties of the as-fabricated membranes

For example, the tensile strength of the CS/KO membrane is about 2.5 times higher than that of the CS membrane. This result can be described by two phenomena. First, the KO particles disperse uniformly in the CS matrix, and act as a reinforcing filler by strengthening the membrane network. Second, the higher tensile strength value is also due to the presence of H bonding created between the polymer matrix and silicate layers, and to the electrostatic interactions between the protonated amino groups of the CS backbone and the anionic groups of mineral particles, as previously reported [17]. Representative stress-strain curves for non-cross-linked and cross-linked membranes are shown in Fig. 9. It can be seen that the PEG and CA incorporation into the casting slurry resulted in an opposite change in mechanical properties compared to the CS/KO membrane. For the non-cross-linked membrane, the tensile stress was found to be slightly lower than that of CS/KO, while for the cross-linked sample, it was much higher. In contrast, the elongation at break of the membrane decreased about twofold by the formation of cross-linking points. These results are probably explained by following reasons. The tensile strength of the membranes was reduced by the introduction of the polymeric pore-forming agent because the insertion of the PEG molecules into the membrane matrix increases the free volume and the molecular mobility of the polymer chains. At the same time, the elongation at break of membranes is strongly enhanced. The values obtained in the current work are in agreement with the trend followed by the studies performed so far. The intercalation of PEG molecules into the membrane matrix leads to the weakening of inter-chain interactions and thus acts as a plasticizer. As a result, the elongation at break increased and the tensile strength decreased [19, 48].

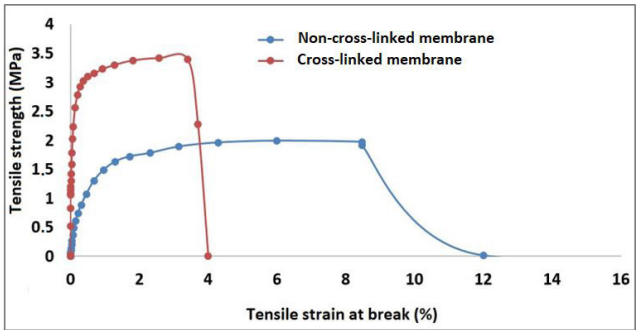

Fig. 9 Tensile test of non-cross-linked and cross-linked composite membranes

Among the different membranes prepared, the cross-linked membrane showed the highest values of tensile strength. The improved mechanical property can be attributed to the CA cross-linking reaction, which induces a higher Young's modulus of these materials (Fig. 9). However, a different trend is observed for elongation at break for cross-linked membrane, since it strongly decreased by about a factor 2 compared to that of the non-cross-linked membrane (Fig. 9). The high amounts of inter-chained bonds between CS and CA are assumed to reduce the flexibility and mobility of the polymer chains resulting in decreased membrane plasticity. In addition, the strong ionic interaction between the negatively charged CA carboxylate groups and the positively charged CS amino groups hinders the free movement of polymeric chains resulting in a more brittle material. To conclude, CA cross-linking results in a membrane material with good mechanical properties in terms of Young's modulus and tensile strength that make it suitable for the operating filtration experiments.

3.2.5 Thermal stability study

The thermal stability of the prepared membranes was determined by TGA. For all composite samples, the thermograms can be generally divided into three regions. From the TGA and DTG curves, onset temperatures for different stages of decomposition, final residue in weight %, and weight loss (%) at each step of degradation are calculated and summarized in Table 2. As shown in Fig. 10, the CS/KO membrane underwent three-stage weight losses with temperatures of 70 °C, 287 °C, and 493 °C. The first stage is most likely due to the evaporation of the

Table 2 TGA data of the different prepared membranes

Sample designation	Onset temperature of degradation (°C)			Weight loss (%)			Residue at 800 °C (wt%)
	First	Second	Third	First	Second	Third	
CS [17]	100	280	330–550	9	49	40	2
CS/KO [18]	70	287	493	3	23	30	44
CS/KO/PEG [18]	70	298	569	3.5	32.5	31	33
CS/KO/PEG/CA	47	270	511	3	21	18	58

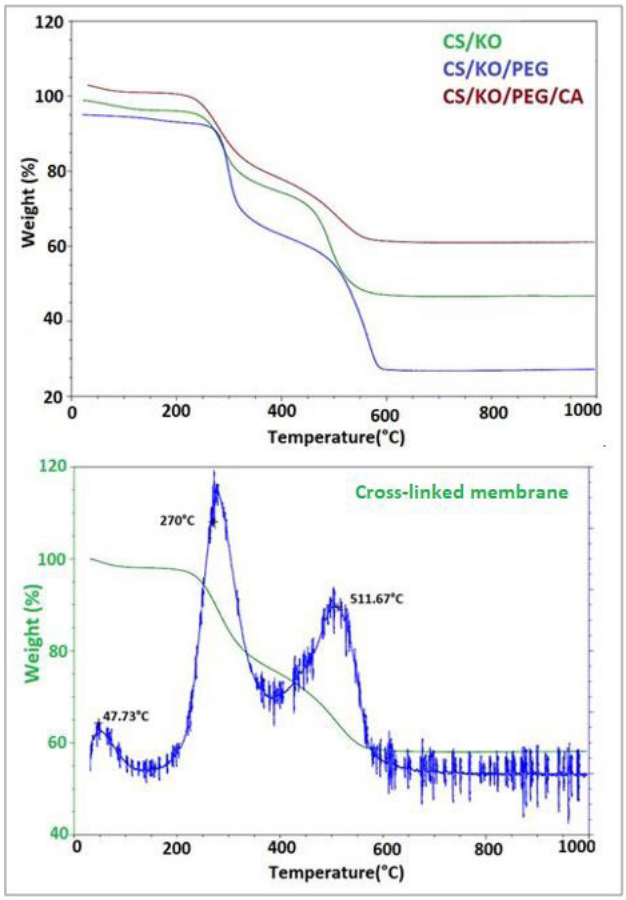

Fig. 10 TGA curves of CS/KO, non-cross-linked and CA-cross-linked membranes

physically adsorbed water, whereas the second stage corresponds to the primary decomposition of CS. The third stage is mainly due to the phenomenon of dehydroxylation of kaolinite and the complete degradation of CS backbone at high temperature [17, 18]. Three weight losses were also observed in the TGA curve for the non-cross-linked membrane (CS/KO/PEG). As before, the first one was attributed to the evaporation of sorbed water. A comparison of the TGA curves suggests that there was no obvious difference between these two membranes in the last stage which is ascribed to the decomposition of CS and KO. However, in the range of 200–400 °C, the weight loss was more marked with the addition of PEG. It can be concluded that the large weight loss at a temperature of about 298 °C is related to the partial decomposition of CS and PEG chains. The incorporation of the polymer additive slightly increased the thermal stability of the CS/KO/PEG membrane compared to the CS/KO membrane with a decomposition onset temperature about 10 °C higher (Table 2). The weight loss of the composite membranes at 800 °C increased from 55% to 66% for CS/KO and CS/KO/PEG, respectively. This observation can be attributed to the PEG–CS interaction that weakens the strong intermolecular bonds between both CS-CS chains and CS-KO and, therefore, the high temperature decomposition rate of the CS/KO/PEG membrane is higher than that of CS-KO sample although it starts at higher temperature (Table 2). The addition of CA to the composite membrane resulted in differences in the thermal stability properties between the non-cross-linked and cross-linked membranes. When comparing their thermal stability, a small shift in the onset of decomposition temperatures was noted from 298 to 270 °C and from 569 to 511 °C as a consequence of CA cross-linking. As can be seen in Fig. 10, there is a slight weight loss (approximately 3%) between 30–150 °C, which can be associated to the dehydration of the membrane as indicated previously for the other membranes. The second stage occurs with a weight loss of 21%. The final decline occurred between 350–600 °C surprisingly accounting for a weight loss of only 18%. Thus, it can be concluded from the TGA data that the ionic cross-linking reaction of CS by CA increased the stability of the CS/KO network at high temperature. This effect suggests that the formed electrostatic cross-linking bonds between the CS chains take place within the CS/KO network and may involve KO.

3.2.6 Chemical stability

Resistance to water washout is an important parameter to be considered for the use of these membranes in water treatment applications. Therefore, in this paper, the water solubilization of the pure CS membrane and all composite membranes under different pH conditions was investigated to study their chemical stability under the operating

conditions by scanning a wide pH range. According to the results presented in Table 3, all composite membranes exhibited a significant increase in chemical stability compared to the neat CS film. The results show that the pure CS membrane has a poor chemical stability and dissolve in water and in acid environment, as expected. On the other hand, the CS/KO composite membrane retains its original state in deionized water, revealing the importance of the KO association with the CS chain in preventing polymer dissolution through the formation of three-dimensional networks involving interactions between the clay and the polymer. Although KO is not a cross-linking agent strictly speaking, the interactions in the matrix are strong enough to maintain the CS/KO composite in a physically cross-linked state that practically prevents the membrane dissolution in water at natural pH. However, the prepared membranes were found to be completely soluble in an acidic medium (pH = 4). It becomes clear that improving the composite membrane stability in acidic medium should be done for practical applications. Investigations have proven that modification of CS in term of cross-linking is crucial to stabilize its chemical stability [26]. The formation of cross-linking bonds between CS polymer chains was also confirmed by the solubility characteristics of membranes before and after reaction with CA. Before cross-linking, the membrane was readily dissolved in an acidic solution at pH = 4, but after cross-linking, it can resist in the same acidic solution, which confirms the role played by CA in the membrane chemical stabilization. This was again due to the compact network formed by high amounts of electrostatic interchain bonds between CS and CA. It is thus shown that the formation of a three-dimensional network structure was responsible initially for an increase in the viscosity of the casting solution (Fig. 2) and then for an enhancement in the physical properties of the obtained composite membranes (Figs. 9, 10, Table 3). The improvement in acid stability with cross-linking is likely related to a decrease in the number of available amine groups and to the loss of chain mobility resulting in fully insoluble membranes. In conclusion, the beneficial protective effect of the clay particles and the cross-linking reaction was demonstrated. This feature makes CS/KO/PE/CA membranes particularly suitable for application in water treatment.

Table 3 Solubility effect of pure and composite chitosan membranes

	CS	CS/KO	CS/KO/PEG	CS/KO/PEG/CA
pH = 9	Insoluble	Insoluble	Insoluble	Insoluble
pH = 6.2	Soluble	Insoluble	Insoluble	Insoluble
pH = 4	Soluble	Soluble	Soluble	Insoluble

3.3 Membrane performance evaluation

For most membrane application, permeability and selectivity are two key parameters. Different characterization parameters such as pure water flux (PWF), pure water permeability (PWP) and MWCO were used to evaluate the performances of the composite membranes prepared. PWP was determined from the slope of PWF as a function of applied pressure (Fig. 11). Compared to the pristine CS membrane, the water permeability of all composite membranes increased (Fig. 12). Addition of a porogen to the CS/KO base composite membrane leads to a large increase in permeability (about 7-fold) and about two orders of magnitude compared to the pure CS membrane. These data are in excellent agreement with the observed morphology changes. The neat CS membrane exhibited the lowest permeability, due to its dense structure and the lack of porosity.

The introduction of inorganic fillers leads to an increase in PWP compared to the pristine membrane, which can be explained by the formation of tiny pores at the surface of CS/KO membrane as it can be seen in Fig. 3, thus improving the water permeability. The extremely high PWP observed when PEG was added to the casting solution was due to the increased hydrophilicity of the membrane surface (Fig. 6) and to the increased density and size of the

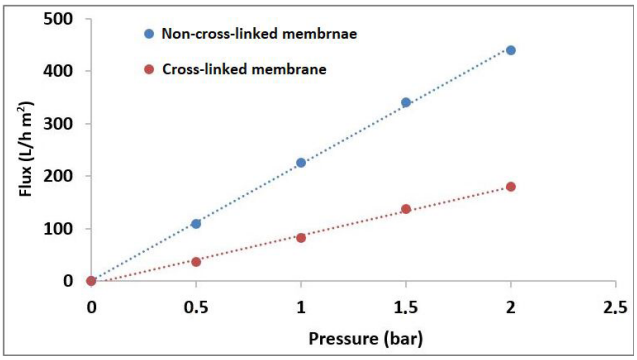

Fig. 11 Water flux permeability versus operating pressure for non-cross-linked and cross-linked membranes

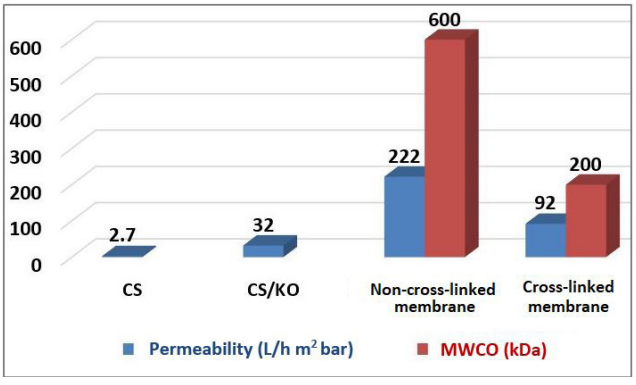

Fig. 12 PWP and MWCO values of obtained membranes

surface pores (Figs. 4 and 7). This could also be explained by the finger-like structure observed in the cross-sectional images, which definitely facilitates solution transfer. These factors lowered the resistance of water transfer across the membranes, which improved the membrane permeability as previously discussed. Similar results have also been reported for the incorporation of PEG as an additive in the case of polyamide membranes [46]. MWCO of the CS/KO/PEG membrane, being determined using filtration of PEG and PEO of different molecular weights, confirms the pore size measurement after SEM observations (Fig. 5).

Fig. 11 shows the effect of cross-linking treatment with CA on PWP and MWCO values (CS/KO/PEG/CA membrane). A decrease of the two parameters compared to those of the non-cross-linked membrane was observed. Again these findings are in excellent agreement with the SEM observations and the pore size determination. As shown in Fig. 5, cross-linking results in a two-fold decrease in pore diameter, which consequently lead to a decrease in PWP. It is generally accepted that permeate flux depends on the porosity, pore inter-connection, surface pore size, skin thickness and hydrophilicity of the membranes [49]. Then, the decrease in PWP after the cross-linking step can also be explained by a thickening of the membrane and a higher tortuosity compared to those of the non-cross-linked membrane as observed by SEM (Fig. 4).

An excellent correlation was found between the PWP and MWCO data determined for the corresponding membranes clearly indicating that the cross-linking with CA results in a progressive pore size decrease [7]. The pore narrowing leads to a better selectivity of the cross-linked membranes from the range of microfiltration to that of ultrafiltration. This observation is in agreement with the PWP values calculated from the PWF data indicating that the cross-linked membrane operated in the ultrafiltration range. On the other hand, the decrease in permeability related to an increase in membrane thickness and tortuosity usually also induces an increase in membrane rejection [42]. As shown in Fig. 11, PWF of cross-linked and non-cross-linked composite membranes varies linearly with the applied pressure in the studied range indicating very good stability of the materials during filtration. PWP of the cross-linked membrane was found to be 2.4-fold lower that the corresponding non-cross-linked membrane. Clearly, the cross-linked composite membrane presented a more pronounced barrier to the transfer of water molecules, resulting in a decrease in PWF. This result was expected because it is well known that any cross-linking procedure reduces the inherent hydrophilicity of CS since the hydrophilic amine groups are consumed to achieve cross-linking. In addition, cross-linking led to a more compact membrane surface structure due to the contraction of pore size [7].

4 Conclusion

In conclusion, we successfully designed novel composite membrane based on chitosan with KO filler, PEG pore forming agent and citric acid cross-linker. A significant improvement in the properties of the neat chitosan film was obtained with these mixed matrix membranes. First, the introduction of KO particles resulted in a strong enhancement of thermal, mechanical and chemical stability properties of the resulting membranes. Second, the study revealed that the introduction of PEG into the slurry formulation not only significantly increased the membrane porosity but also the hydrophilicity of the membrane surface. Both factors contribute to the strong increase in water permeance. Lastly, the solubility of membrane in acidic media was prevented by its cross-linking with citric acid as a green cross-linker. The cross-linked membrane exhibited good mechanical, thermal and chemical stability, making it suitable for application in water treatment. CA not only contributed to CS cross-linking but also to pore constriction thus improving the functional selectivity properties of the membrane. Based on these observations, it was concluded that the prepared cross-linked membrane exhibited quite good properties with potential application in ultrafiltration.

Acknowledgement

The authors are grateful to the Ministry of Education Tunisia for the S. B. Rekik's stay in France for the financial assistance provided through the *Bourse d'alternance* (work-study grant) program. Work at the *Institut Européen des Membranes* (European Institute of Membranes) was supported by institutional funding from CNRS, ENSCM and University of Montpellier.

References

[1] Takht Ravanchi, M., Kaghazchi, T., Kargari., A. "Application of membrane separation processes in petrochemical industry: a review", Desalination, 235(1–3), pp. 199–244, 2009. https://doi.org/10.1016/j.desal.2007.10.042

[2] Pendergast, M. M., Hoek, E. M. V. "A review of water treatment membrane nanotechnologies", Energy & Environmental Science, 4(6), pp. 1946–1971, 2011. https://doi.org/10.1039/C0EE00541J

[3] Biscarat, J., Charmette, C., Sanchez, J., Pochat-Bohatier, C. "Preparation of dense gelatin membranes by combining temperature induced gelation and dry-casting", Journal of Membrane Science, 473, pp. 45–53, 2015.
https://doi.org/10.1016/j.memsci.2014.09.004

[4] Carneiro, R. T. A., Taketa, T. B., Gomes Neto, R. J., Oliveira, J. L., Campos, E. V. R., de Moraes M. A., da Silva, C. M. G., Beppu, M. M., Fraceto, L. F. "Removal of glyphosate herbicide from water using biopolymer membranes", Journal of Environmental Management, 151, pp. 353–360, 2015.
https://doi.org/10.1016/j.jenvman.2015.01.005

[5] Kamal, O., Pochat-Bohatier, C., Sanchez-Marcano, J. "Development and stability of gelatin cross-linked membranes for copper (II) ions removal from acid waters", Separation and Purification Technology, 183, pp. 153–161, 2017.
https://doi.org/10.1016/j.seppur.2017.04.007

[6] No, H. K., Lee, K. S., Meyers, S. P. "Correlation between physicochemical characteristics and binding capacities of chitosan products", Journal of Food Science, 65(7), pp. 1134–1137, 2000.
https://doi.org/10.1111/j.1365-2621.2000.tb10252.x

[7] Cheung, R. C. F., Ng, T. B., Wong, J. H., Chan, W. Y. "Chitosan: An update on potential biomedical and pharmaceutical applications", Marine Drugs, 13(8), pp. 5156–5186, 2015.
https://doi.org/10.3390/md13085156

[8] Hamed, I., Özogul, F., Regenstein, J. M. "Industrial applications of crustacean by-products (chitin, chitosan, and chitooligosaccharides): A review", Trends in Food Science & Technology, 48, pp. 40–50, 2016.
https://doi.org/10.1016/j.tifs.2015.11.007

[9] Hamedi, H., Moradi, S., Hudson, S. M., Tonelli, A. E., King, M. W. "Chitosan based bioadhesives for biomedical applications: A review", Carbohydrate Polymers, 282, 119100, 2022.
https://doi.org/10.1016/j.carbpol.2022.119100

[10] Kumar, R., Isloor, A. M., Ismail, A. F., Matsuura, T. "Synthesis and characterization of novel water soluble derivative of chitosan as an additive for polysulfone ultrafiltration membrane", Journal of Membrane Science, 440, pp. 140–147, 2013.
https://doi.org/10.1016/j.memsci.2013.03.013

[11] Lavorgna, M., Attianese, I., Buonocore, G. G., Conte, A., Del Nobile, M. A., Tescione, F., Amendola, E. "MMT-supported Ag nanoparticles for chitosan nanocomposites: Structural properties and antibacterial activity", Carbohydrate Polymers, 102, pp. 385–392, 2014.
https://doi.org/10.1016/j.carbpol.2013.11.026

[12] Cooper, A., Floreani, R., Ma, H., Bryers, J. D., Zhang, M. "Chitosan-based nanofibrous membranes for antibacterial filter applications", Carbohydrate Polymers, 92(1), pp. 254–259, 2013.
https://doi.org/10.1016/j.carbpol.2012.08.114

[13] Uragami, T., Saito, T., Miyata, T. "Pervaporative dehydration characteristics of an ethanol/water azeotrope through various chitosan membranes", Carbohydrate Polymers, 120, pp. 1–6, 2015.
https://doi.org/10.1016/j.carbpol.2014.11.032

[14] Prasad, N. S., Moulik, S., Bohra, S., Rani, K. Y., Sridhar, S. "Solvent resistant chitosan/poly(ether-*block*-amide) composite membranes for pervaporation of *n*-methyl-2-pyrrolidone/water mixtures", Carbohydrate Polymers, 136, pp. 1170–1181, 2016.
https://doi.org/10.1016/j.carbpol.2015.10.037

[15] Liu, Q., Zhao, Y., Pan, J., Van der Bruggen, B., Shen, J. "A novel chitosan base molecularly imprinted membrane for selective separation of chlorogenic acid", Separation and Purification Technology, 164, pp. 70–80, 2016.
https://doi.org/10.1016/j.seppur.2016.03.020

[16] Salehi, E., Khajavian, M., Sahebjamee., N., Mahmoudi, M., Drioli, E., Matsuura, T. "Advances in nanocomposite and nanostructured chitosan membrane adsorbents for environmental remediation: a review", Desalination, 527, 115565, 2022.
https://doi.org/10.1016/j.desal.2022.115565

[17] Rekik, S. B., Gassara, S., Bouaziz, J., Deratani, A., Baklouti, S. "Development and characterization of porous membranes based on kaolin/chitosan composite", Applied Clay Science, 143, pp. 1–9, 2017.
https://doi.org/10.1016/j.clay.2017.03.008

[18] Rekik, S. B., Gassara, S., Bouaziz, J., Deratani, A., Baklouti, S. "Enhancing hydrophilicity and permeation flux of chitosan/kaolin composite membranes by using polyethylene glycol as porogen", Applied Clay Science, 168, pp. 312–323, 2019.
https://doi.org/10.1016/j.clay.2018.11.029

[19] Priyadarshi, R., Sauraj, Kumar, B., Negi, Y. S. "Chitosan film incorporated with citric acid and glycerol as an active packaging material for extension of green chilli shelf life", Carbohydrate Polymers, 195, pp. 329–338, 2018.
https://doi.org/10.1016/j.carbpol.2018.04.089

[20] Pankaj, G., Ashim, J. T., Rashmi, R. D., Bodhaditya, D., Tarun, K. M. "A comparative study on sorption of arsenate ions from water by crosslinked chitosan and crosslinked chitosan/MMT nanocomposite", Journal of Environmental Chemical Engineering, 4(4), pp. 4248–4257, 2016.
https://doi.org/10.1016/j.jece.2016.09.027

[21] Yan, E., Cao, M., Wang, Y., Hao, X., Pei, S., Gao, J., Wang, Y., Zhang, Z., Zhang, D. "Gold nanorods contained polyvinyl alcohol/chitosan nanofiber matrix for cell imaging and drug delivery", Materials Science and Engineering: C, 58, pp. 1090–1097, 2016.
https://doi.org/10.1016/j.msec.2015.09.080

[22] de Y. Pozzo, L., da Conceição, T. F., Spinelli, A., Scharnagl, N., Pires, A. T. N. "Chitosan coatings crosslinked with genipin for corrosion protection of AZ31 magnesium alloy sheets", Carbohydrate Polymers, 181, pp. 71–77, 2018.
https://doi.org/10.1016/j.carbpol.2017.10.055

[23] Ghalia, M. A., Abdelrasoul, A. "7 - Synthesis and characterization of biopolymer-based mixed matrix membranes", In: Verma, D., Fortunati, E., Jain, S., Zhang, X. (eds.) Biomass, Biopolymer-Based Materials, and Bioenergy: Construction, Biomedical, and other Industrial Applications, Woodhead Publishing, pp. 123–134, 2019. ISBN 978-0-08-102426-3
https://doi.org/10.1016/B978-0-08-102426-3.00007-2

[24] Sapna, Sharma, R., Kumar, D. "Chapter 29 - Chitosan-based membranes for wastewater desalination and heavy metal detoxification", In: Thomas, S., Pasquini, D., Leu, S.-Y., Gopakumar, D. A. (eds.) Nanoscale Materials in Water Purification, Elsevier, pp. 799–814, 2019. ISBN 978-0-12-813926-4
https://doi.org/10.1016/B978-0-12-813926-4.00037-9

[25] Ahmed, M. J., Hameed, B. H., Hummadi, E. H. "Review on recent progress in chitosan/chitin-carbonaceous material composites for the adsorption of water pollutants", Carbohydrate Polymers, 247, 116690, 2020.
https://doi.org/10.1016/j.carbpol.2020.116690

[26] Grzybek, P., Jakubski, Ł., Dudek, G. "Neat Chitosan Porous Materials: A Review of Preparation, Structure, Characterization and Application", International Journal of Molecular Sciences, 23(17), 9932, 2022.
https://doi.org/10.3390/ijms23179932

[27] Shchipunov, Y. A., Silant'ev, V. E., Postnova, I. V. "Self-organization in the chitosan–clay nanoparticles system regulated through polysaccharide macromolecule charging. 1. Hydrogels", Colloid Journal, 74(5), pp. 636–644, 2012.
https://doi.org/10.1134/S1061933X12050092

[28] Huang, Y., Huang, J., Cai, J., Lin, W., Lin, Q., Wu, F., Luo, J. "Carboxymethyl chitosan/clay nanocomposites and their copper complexes: Fabrication and property", Carbohydrate Polymers, 134, pp. 390–397, 2015.
https://doi.org/10.1016/j.carbpol.2015.07.089

[29] de Costa, M. P. M., de Mello Ferreira, I. L., de Macedo Cruz, M. T. "New polyelectrolyte complex from pectin/chitosan and montmorillonite clay", Carbohydrate Polymers, 146, pp. 123–130, 2016.
https://doi.org/10.1016/j.carbpol.2016.03.025

[30] Wang, B., Jackson, E. A., Hoff, J. W., Dutta, P. K. "Fabrication of zeolite/polymer composite membranes in a roller assembly", Microporous and Mesoporous Materials, 223, pp. 247–253, 2016.
https://doi.org/10.1016/j.micromeso.2015.11.003

[31] Anaya-Esparza, L. M., Vargas-Torres, A., Palma-Rodríguez, H. M., Castro-Mendoza, M. P., Yahia, E. M., Pérez-Larios, A., Montalvo-González, E. "Effect of Mixed Oxide-Based TiO_2 on the Physicochemical Properties of Chitosan Films", Periodica Polytechnica Chemical Engineering, 66(3), pp. 422–436, 2022.
https://doi.org/10.3311/PPch.18953

[32] Dey, S. C., Al Amin, M., Rachid, T. U., Ashaduzzaman, M., Md Shamsuddin, S. "pH induced fabrication of kaolinite-chitosan biocomposite", International Letters of Chemistry, Physics and Astronomy, 68, pp. 1–9, 2016.
https://doi.org/10.18052/www.scipress.com/ILCPA.68.1

[33] Sun, X., Tang, Z., Pan, M., Wang, Z., Yang, H., Liu, H. "Chitosan/kaolin composite porous microspheres with high hemostatic efficacy", Carbohydrate Polymers, 177, pp. 135–143, 2017.
https://doi.org/10.1016/j.carbpol.2017.08.131

[34] Shenvi, S., Ismail, A. F., Isloor, A. M. "Preparation and characterization study of PPEES/chitosan composite membrane crosslinked with tripolyphosphate", Desalination, 344, pp. 90–96, 2014.
https://doi.org/10.1016/j.desal.2014.02.026

[35] Gierszewska, M., Ostrowska-Czubenko, J. "Chitosan-based membranes with different ionic crosslinking density for pharmaceutical and industrial applications", Carbohydrate Polymers, 153, pp. 501–511, 2016.
https://doi.org/10.1016/j.carbpol.2016.07.126

[36] Salehi, E., Madaeni, S. S. "Influence of poly(ethylene glycol) as pore-generator on morphology and performance of chitosan/poly(vinyl alcohol) membrane adsorbents", Applied Surface Science, 288, pp. 537–541, 2014.
https://doi.org/10.1016/j.apsusc.2013.10.067

[37] Sharma, N., Purkait, M. K. "Impact of synthesized amino alcohol plasticizer on the morphology and hydrophilicity of polysulfone ultrafiltration membrane", Journal of Membrane Science, 522, pp. 202–215, 2017.
https://doi.org/10.1016/j.memsci.2016.08.068

[38] Bagheri, M., Younesi, H., Hajati, S., Borghei, S. M. "Application of chitosan-citric acid nanoparticles for removal of chromium (VI)", International Journal of Biological Macromolecules, 80, pp. 431–444, 2015.
https://doi.org/10.1016/j.ijbiomac.2015.07.022

[39] Narayanan, A., Kartik, R., Sangeetha, E., Dhamodharan, R. "Super water absorbing polymeric gel from chitosan, citric acid and urea: Synthesis and mechanism of water absorption", Carbohydrate Polymers, 191, pp. 152–160, 2018.
https://doi.org/10.1016/j.carbpol.2018.03.028

[40] Venault, A., Vachoud, L., Pochat, C., Bouyer, D., Faur, C. "Elaboration of Chitosan/Activated carbon composites for the removal of organic pollutants from waters", Environmental Technology, 29(12), pp. 1285–1296, 2008.
https://doi.org/10.1080/09593330802296256

[41] Céline, P.-B., Antoine, V.,Denis, B., Laurent, V., Laurent, D., Catherine, F. "Development and Characterization of Composite Chitosan/Active Carbon Hydrogels for a Medical Application", Journal of Applied Polymer Science, 128(5), pp. 2945–2953, 2013.
https://doi.org/10.1002/app.38414

[42] Gassara, S., Chinpa, W., Quemener, D., Ben Amar, R., Deratani, A. "Pore size tailoring of poly (ether imide) membrane from UF to NF range by chemical post-treatment using aminated oligomers", Journal of Membrane Science, 436, pp. 36–46, 2013.
https://doi.org/10.1016/j.memsci.2013.02.005

[43] Nasri, H., Khemakhem, S., Amar, R. B. "Physico-Chemical Study of Coating Formulation Based on Natural Apatite for the Elaboration of Microfiltration Membrane", Periodica Polytechnica Chemical Engineering, 58(2), pp. 171–178, 2014.
https://doi.org/10.3311/PPch.7388

[44] Rekik, S. B., Bouaziz, J., Deratani, A., Baklouti, S. "Development of an asymmetric ultrafiltration membrane from naturally-occurring kaolin clays: Application to the cuttlefish effluents treatments", Journal of Membrane Science & Technology, 6(3), 1000159, 2016.
https://doi.org/10.4172/2155-9589.1000159

[45] M'barki, O., Hanafia, A., Bouyer, D., Faur, C., Sescousse, R., Delabre, U., Blot, C., Guenoun, P., Deratani, A., Quemener, D. Pochat-Bohatier, C. "Greener method to prepare porous polymer membranes by combining thermally induced phase separation and crosslinking of poly (vinyl alcohol) in water", Journal of Membrane Science, 458, pp. 225–235, 2014.
https://doi.org/10.1016/j.memsci.2013.12.013

[46] You, X., Ma, T., Su, Y., Wu, H., Wu, M., Cai, H., Sun, G., Jiang, Z. "Enhancing the permeation flux and antifouling performance of polyamide nanofiltration membrane by incorporation of PEG-POSS nanoparticles", Journal of Membrane Science, 540, pp. 454–463, 2017.
https://doi.org/10.1016/j.memsci.2017.06.084

[47] Quéré, D. "Wetting and roughness", Annual Review of Materials Research, 38, pp. 71–99, 2008.
https://doi.org/10.1146/annurev.matsci.38.060407.132434

[48] Sanyang, M. L., Sapuan, S. M., Jawaid, M., Ishak, M. R., Sahari, J. "Effect of Plasticizer Type and Concentration on Tensile, Thermal and Barrier Properties of Biodegradable Films Based on Sugar Palm (*Arenga pinnata*) Starch", Polymers, 7(6), pp. 1106–1124, 2015. https://doi.org/10.3390/polym7061106

[49] Tran, D.-T., Mendret, J., Méricq, J.-P., Faur, C., Brosillon, S. "Study of Permeate Flux Behavior during Photo-Filtration Using Photocatalytic Composite Membranes", Chemical Engineering and Processing - Process Intensification, 148, 107781, 2020. https://doi.org/10.1016/j.cep.2019.107781